Late Pleistocene and Holocene activity of the Atacazo-Ninahuilca Volcanic Complex (Ecuador)

Hidalgo, Silvana; Monzier, Michel; Almeida, Eduardo; Chazot, Gilles; Eissen, Jean-Philippe; van der Plicht, Johannes; Hall, Minard L.

Published in:
Journal of Volcanology and Geothermal Research

DOI:
10.1016/j.jvolgeores.2008.05.017

Publication date:
2008

Journal of Volcanology and Geothermal Research 176 (2008) 16–26

Contents lists available at ScienceDirect

Journal of Volcanology and Geothermal Research

journal homepage: www.elsevier.com/locate/jvolgeores

Late Pleistocene and Holocene activity of the Atacazo–Ninahuilca Volcanic Complex (Ecuador)

Silvana Hidalgo [a,b,*], Michel Monzier [c,1], Eduardo Almeida [d], Gilles Chazot [b], Jean-Philippe Eissen [c,1], Johannes van der Plicht [e], Minard L. Hall [a]

[a] Instituto Geofísico, Escuela Politécnica Nacional, A.P. 17-01-2759, Quito, Ecuador
[b] Laboratoire Magmas et Volcans, CNRS UMR 6524, 5 rue Kessler, 63038 Clermont-Ferrand, France
[c] Institut de Recherche pour le Développement, Laboratoire Magmas et Volcans, IRD UMR 163, 5 rue Kessler, 63038 Clermont-Ferrand, France
[d] Caminosca Cia. Ltda. Quito, Ecuador
[e] Center for Isotope Research, University of Groningen, Nijenborgh 4, 9747 AG Groningen, Netherlands, and Faculty of Archaeology, University of Leiden, PO Box 9515, 2300 RA Leiden, Netherlands

ARTICLE INFO

Article history:
Received 1 November 2006
Accepted 26 May 2008
Available online 3 June 2008

Keywords:
Atacazo–Ninahuilca
Ecuador
Holocene
stratigraphy
geochronology
radiocarbon dating
volcanic hazards

ABSTRACT

The Atacazo–Ninahuilca Volcanic Complex (ANVC) is located in the Western Cordillera of Ecuador, 10 km southwest of Quito. At least six periods of Pleistocene to Holocene activity (N1 to N6) have been preserved in the geologic record as tephra fallouts and pyroclastic flow deposits. New field data, including petrographic and whole-rock geochemical analyses of over forty soil and tephra sections, 100 pumice and lithic samples, and 10 new ^{14}C ages allow us to constrain: (1) the tephra fall isopachs and detailed characteristics of the last two events (N5–N6) including volume estimates of the tephra and pyroclastic flow deposits and the corresponding volcanic explosivity index (VEI); (2) the petrographical and geochemical correlations between domes, tephras, and pyroclastic flow deposits; and, (3) the timing of the last 4 eruptive events and a period of quiescence that endured a few thousand years (1000–4000).
The last two eruptive events (N5 and N6) took place at around 4400±35 yr BP and 2270±15 yr BP, producing huge plinian and pyroclastic flow deposits. Taking into account the widely spread deposits of these VEI 5 eruptions, the present population of about 70000 people, and the current infrastructure; the development of mitigation plans and deployment of monitoring systems at ANVC is highly recommended.

1. Introduction

More than sixty Quaternary volcanic complexes comprise the Ecuadorian Volcanic Arc (Fig. 1). Of these, at least seventeen have been active during the Holocene, and eight produced historical eruptions. This situation has prompted the reconstruction of the volcanic stratigraphy for numerous volcanoes throughout the Andean range, and the elaboration of hazard maps for most active and dangerous edifices (Hall, 1977; Barberi et al., 1988; Hall and Beate, 1991; Hall and Maruri, 1992; Hall and Mothes, 1994; Samaniego et al., 1998; Barba et al., 2008-this issue). During the last decade, Guagua Pichincha, Tungurahua, and Reventador volcanoes erupted, endangering Ecuadorian populations and infrastructures of high economic importance (such as the trans-Ecuadorian oil pipeline). This volcanic activity led to important human conflicts, and challenged the local and regional authorities.

The Atacazo–Ninahuilca Volcanic Complex (ANVC), the focus of this study, is located in the Western Cordillera of Ecuador (volcanic front), 10 km southwest of Quito (Fig. 1). Explosive activity at ANVC during the Holocene produced thick tephra layers and huge pyroclastic flow deposits that have traveled several kilometers westward from the vent. South of Quito, several small towns (*e.g.* Tambillo, Uyumbicho, Aloag, Tandapi, Canchacoto), the main Panamerican highway, crossing the highland area from north to south, and the road leading from Aloag to Santo Domingo, linking the Northern highlands to the Coastal region; were built upon recent Holocene eruptive deposits, and are now positioned in high hazard zones. In the event of a reactivation of the ANVC, at least 70000 people (INEC, 2001), the National Electrical System, and Quito's water supply could be adversely affected.

In order to better constrain the eruptive style and frequency of the ANVC, a stratigraphic, petrographic, geochemical, and chronological study was undertaken. Forty stratigraphic sections containing fallout and flow deposits related to the ANVC late Pleistocene to Holocene activity were studied mainly to the east and southwest of the complex. Carbonized wood and charred twigs found inside pyroclastic flow deposits or organic-rich paleosoils related to plinian fallout layers

* Corresponding author. Instituto Geofísico, Escuela Politécnica Nacional, A.P. 17-01-2759, Quito, Ecuador.
E-mail address: shidalgo@igepn.edu.ec (S. Hidalgo).
[1] Deceased.

0377-0273/$ – see front matter © 2008 Elsevier B.V. All rights reserved.
doi:10.1016/j.jvolgeores.2008.05.017

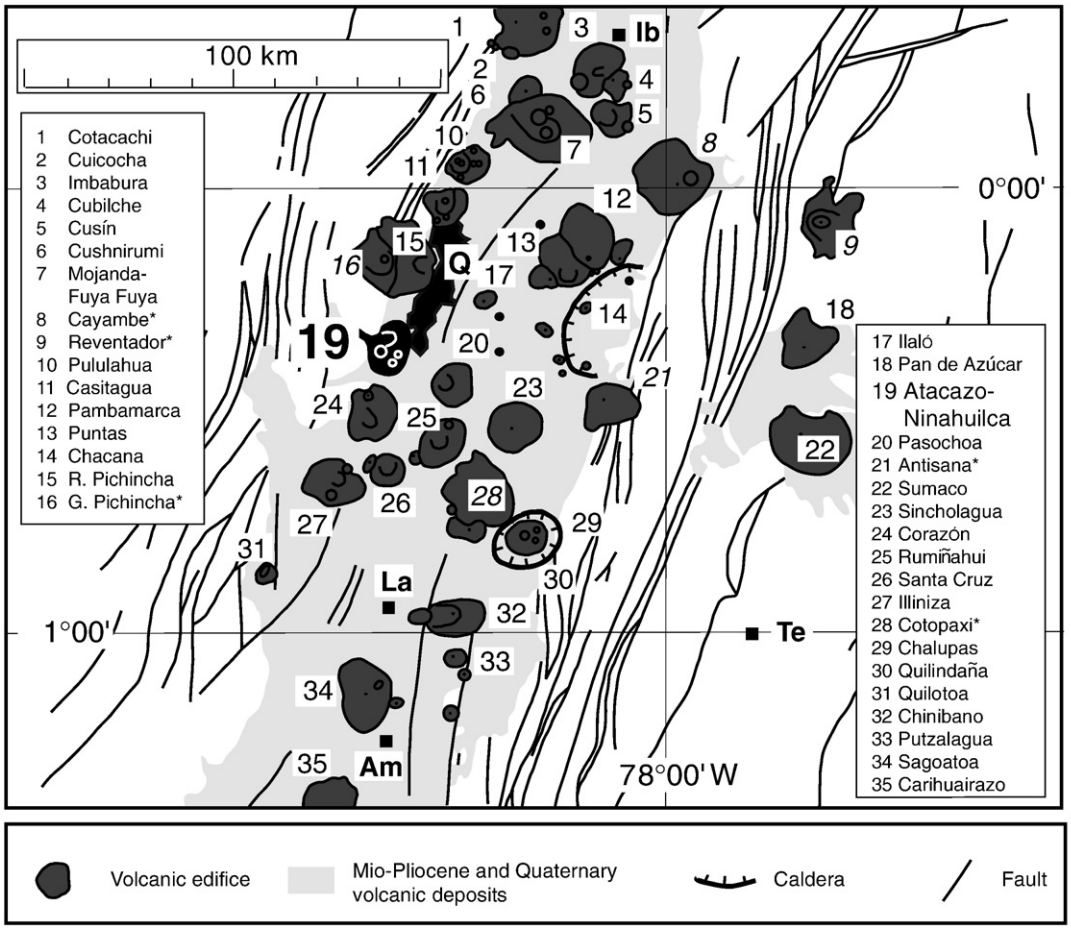

Fig. 1. Location of the Atacazo–Ninahuilca Volcanic Complex (ANVC) in the Ecuadorian Volcanic Arc. Volcanic Centers are from Hall and Beate (1991). The cities shown on this map are: Ib = Ibarra, Q = Quito, La = Latacunga, Te = Tena, Am = Ambato. * = volcano with historical activity.

were dated by ^{14}C technique at the Center for Isotope Research, University of Groningen, Netherlands (Table 1). The conventional radiocarbon ages were calibrated to calendar years using the OxCal software (Bronk Ramsey, 2003). Average ages for the younger eruptions (N5 and N6 eruptive events; see below) were estimated using the same software. The data obtained from paleosols (N5: SA-38A and N6: SA-38C1) were not used in the average because they represent only minimal or maximal ages for an event, and their accuracy is generally lower than that of carbonized wood. The radiocarbon ages and the calibrated age ranges (confidence levels at 1 and 2 sigma) are listed in Table 1.

Pumice and juvenile lithic fragments used in petrographical and geochemical studies were sampled directly from domes, tephra, and pyroclastic flow deposits. Whole-rock geochemical analyses for major and trace elements were performed at the Université de Bretagne Occidentale, France. Petrographic and geochemical studies were used to establish a correlation between the different Pleistocene and Holocene tephra and pyroclastic flow deposits and their related domes.

2. ANVC — main units: stratigraphy and geochronology of recent deposits

The ANVC can be subdivided into three main edifices: La Carcacha, Atacazo, and a group of recent domes. La Carcacha edifice is the oldest of the complex, composed of andesitic lava flows. The younger Atacazo stratovolcano is made up of several sequences of andesitic lava flows and five satellite domes (Omoturco, Cuscungo, La Viudita, Gallo Cantana, and Arenal I). This edifice underwent a destabilization event that led to the formation of a SW oriented depression (5×7 km). Several late Pleistocene to Holocene domes (La Cocha I and II, Arenal II, Ninahuilca Chico I and II) extruded into this depression (Figs. 2 and 3). At least six periods of explosive activity, defined by Almeida (1996) as N1 to N6, were associated with the formation of these domes. Explosive activity associated with their formation is preserved in the stratigraphic record as six tephra layers, and at least two different pyroclastic flow units cropping out more than 30 km from the vent. The tephra deposits overlie the Late Glacial moraines indicating an age younger than 10–12 ka (cf. Clapperton, 1993).

2.1. Late Pleistocene–Holocene domes

The youngest edifice of the ANVC is a dome complex, composed by five important domes: La Cocha I and II, Arenal II, Ninahuilca Chico I and II.

La Cocha I and II domes (3798 m) are located in the western part of the SW-opened depression of Atacazo edifice (Figs. 2 and 3c). La Cocha I dome was destroyed by an explosive eruption leaving a half-moon shaped structure with a 1.5-km-long scar. This explosive phase was followed by the emplacement of the younger La Cocha II dome. Assuming an original circular shape, the estimated diameter of this dome was likely about 3 km. These lavas contain plagioclase, orthopyroxene, clinopyroxene and Fe–Ti oxides; and have silica contents between 62 and 64 wt.%. An active fumarolic field, about

Table 1
Radiocarbon ages (pre-1950) obtained for carbonized wood, charred twigs and paleosol horizons related to the recent volcanic activity of the Atacazo–Ninahuilca Volcanic Complex

Stratigraphic unit	Dated material	Deposit	Sample number	Radiocarbon age (yr BP)	Calibrate age CalBC 68.2% (1 sigma) (yr BC)	Calibrated age CalBC 95.4% (2 sigma) (yr BC)	Laboratory number	$\delta^{13}C$ (‰)	Cv (%)
N3	Soil	Palaeosoil overlying N3 fallout	SA-67H	8860±70	8210 (60.9%) 7940 7930 (2.2%) 7910 7900 (3.4%) 7870 7860 (1.7%) 7840	8240 (95.4%) 7750	GrN-28732	−25.26	59.1
N4	Charred twigs	Ash flow	Almeida (1996)	5440±111	4440 (2.6%) 4420 4370 (44.4%) 4210 4200 (8.9%) 4160 4150 (1.0%) 4140 4130 (11.3%) 4050	4500 (95.4%) 3990			
N5	Carbonized wood	Pyroclastic Flow	SA-24C	4360±50	3080 (2.1%) 3070 3030 (66.1%) 2900	3270 (1.6%) 3240 3100 (93.8%) 2880	GrN-28725	−27.72	73.8
N5	Carbonized wood	Pyroclastic Flow	SA-24 I	4440±50	3330 (23.8%) 3230 3180 (3.4%) 3150 3120 (32.3%) 3010 2980 (3.5%) 2960 2950 (5.2%) 2920	3340 (39.5%) 3150 3140 (55.9%) 2910	GrN-28726	−25.46	70.90
N5			Average	4400±35	3090 (11.6%) 3060 3040 (59.6%) 2920	3270 (3.2%) 3230 3110 (92.2%) 2910			
N5	Soil	Palaeosoil underlying N5 fallout	SA-38A	4600±40	3500 (30.5%) 3450 3440 (1.2%) 3430 3380 (30.0%) 3330 3210 (3.0%) 3190 3150 (3.5%) 3130	3520 (42.4%) 3400 3390 (34.2%) 3310 3230 (9.1%) 3170 3160 (9.7%) 3100	GrN-28727	−25.46	54.2
N6	Carbonized wood	Pyroclastic flow	SA-42D	2220±40	370 (8.2%) 340 330 (60.0%) 200	390 (95.4%) 170	GrN-28729	−25.51	66.7
N6	Carbonized wood	Pyroclastic flow	SA-52B	2230±40	380 (12.5%) 350 320 (55.7%) 200	390 (95.4%) 190	GrN-28731	−24.87	76.3
N6	Soil	Palaeosoil underlying N6-fallout	SA-38C1	2250±30	390 (24.7%) 350 300 (39.5%) 230 220 (4.0%) 210	400 (30.2%) 340 330 (65.2%) 200	GrN-28728	−22.24	59.9
N6	Carbonized wood	Pyroclastic flow	SA-45B	2260±30	390 (32.1%) 350 290 (36.1%) 230	400 (36.2%) 340 320 (59.2%) 200	GrN-28730	−23.06	68.8
N6	Charred twigs	Palaeosoil	SA-22A	2300±30	400 (59.4%) 360 270 (8.8%) 260	410 (69.1%) 350 300 (26.3%) 230	GrN-28723	−26.09	67.2
N6	Carbonized wood	Pyroclastic flow	SA-22E4	2320±30	410 (67.1%) 370 270 (1.1%) 260	420 (82.4%) 350 290 (13.0%) 230	GrN-28724	−23.33	67.3
N6			Aquater (1980)	2370±70	760 (14.6%) 690 550 (53.6%) 380	800 (90.6%) 350 300 (4.8%) 200			
N6			Average	2267±17	390 (49.1%) 350 280 (19.1%) 260	400 (53.7%) 350 300 (40.4%) 23 220 (1.2%) 210			

The calibrated ages are shown with their 1 and 2 sigma confidence levels. Calculated average ages for N5 and N6 eruptive events are also shown. PF = pyroclastic flow.

50 m in length, was discovered at the foot of the La Cocha II dome. Sulphur crystals, 1 mm in size, coat the orifices of low temperature gas emission vents.

Arenal II dome (4280 m) has a basal diameter of about 1.5 km and a relief of 600 m, with maximum slopes of 23°. This dome has grown along the northern Atacazo depression walls (Fig. 2). The silica content of this lava is 63 wt.%, and the mineral assemblage is comprised of plg+opx+amph+Fe–Ti oxides.

Ninahuilca Chico I (3256 m) is a 1-km-diameter circular dome (500 m-high) located at the southwestern end of the Atacazo depression (Fig. 2). No sample could be obtained from this dome due to difficulties in accessing it. *Ninahuilca Chico II* (3824 m; Figs. 2 and 3c) is an E–W elongated dome (2.5×1.5 km) with a total relief of 700 m. This is less eroded part of the volcanic complex with very steep slopes that are frequently affected by small landslides. The eruptive products have a mineral assemblage of plg+amph+opx+Fe–Ti oxides ±apt. SiO_2 content is quite homogenous ranging around 65 wt.%.

2.2. Tephra deposits

2.2.1. N1 tephra layer

In the upper flanks of the ANVC, the N1 tephra layer is an oxidized 30-cm-thick fine brown ash and pumice layer overlying a 50-cm-thick grayish-red consolidated tuff which is in contact with the older Atacazo lavas. The sequence is overlain by a 35 cm paleosol, poor in organic material. No radiocarbon age could be determined for this layer due to the scarcity of organic or carbonized material. Nevertheless, as it is overlying the Late glacial moraines, this horizon must be younger than 10–12 ka. This layer is exposed about 5 km NE of the Atacazo depression rim (section SA-67, Fig. 4). Based on petrographical or geochemical data, no link with any of the intra-depression domes could be established.

2.2.2. N2 tephra layer

In section SA-67 (Fig. 4), N2 tephra layer is a well-sorted 36-cm-thick fallout containing orange oxidized pumices, fragmented hydrothermally altered lithics, and a fine-grained matrix (plagioclase, pumice, lithics and glass shards). It is overlain by a 55-cm-thick dark paleosol with yellow pumices at the base. Whole-rock analysis from one of N2 tephra layer pumices yields 61 wt.% SiO_2 (Fig. 5), and the mineral assemblage is comprised of plg+opx+Fe–Ti oxides±cpx. As for N1 tephra, no radiogenic age could be obtained for this deposit, however, given its stratigraphic position; it must be younger than 10–12 ka.

2.2.3. N3 tephra layer

In section SA-67, N3 tephra is a 12-cm-thick well-sorted coarse yellow ash layer. It contains 1-cm white/yellow pumices and small (1–2 cm) hydrothermally altered and fragmented lithics. Fine ash, lithics, and plagioclase, Fe–Ti-oxides and orthopyroxene crystals

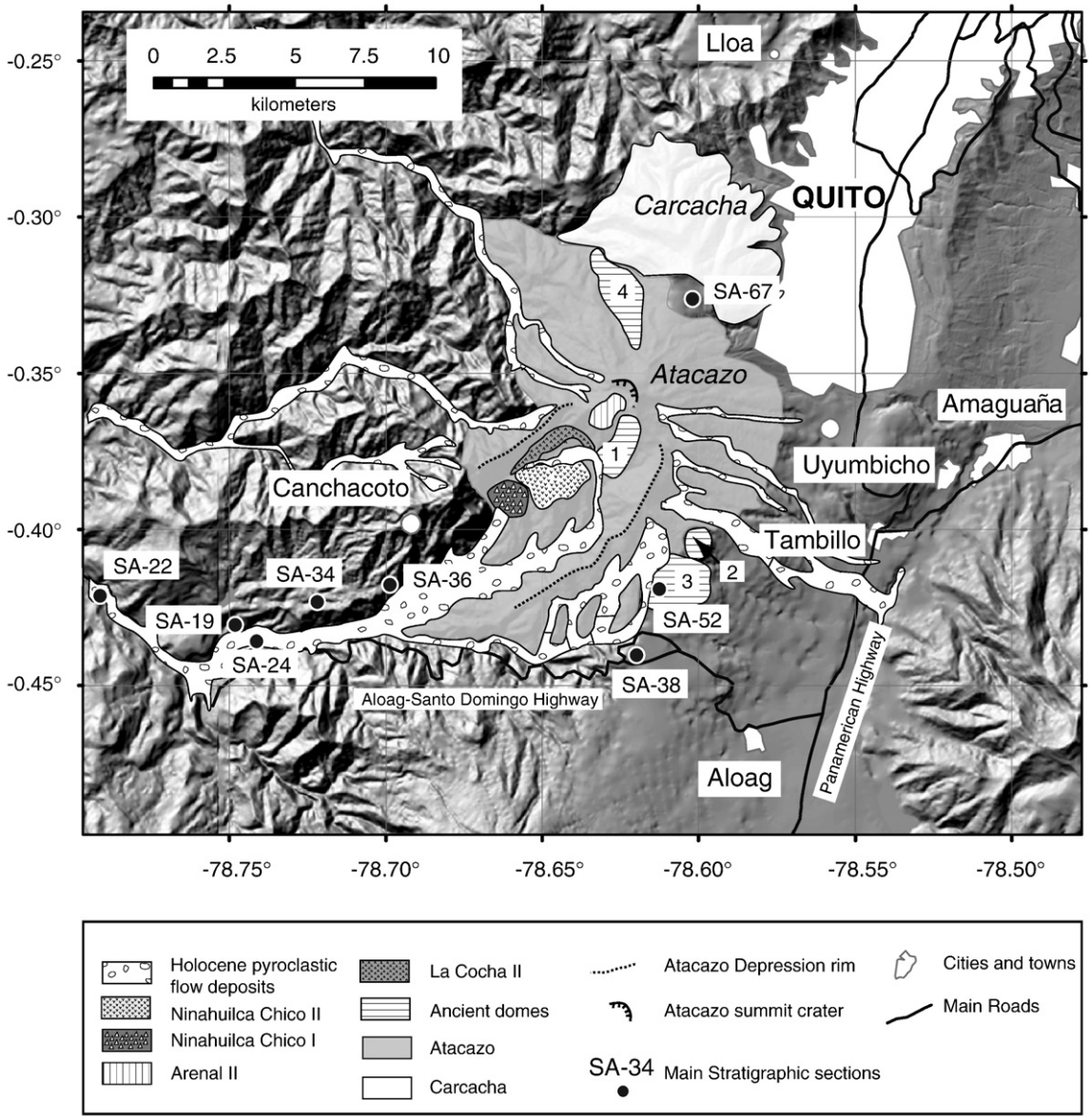

Fig. 2. Schematic map of the geology of the Atacazo–Ninahuilca Volcanic Complex (ANVC), including the older La Carcacha and Atacazo edifices, the Atacazo satellite domes (1 = Arenal I, 2 = Cuscungo, 3 = La Viudita, 4 = Gallo Cantana), and Late Pleistocene–Holocene intra-depression domes. Location of the main stratigraphic sections is also shown.

comprise the matrix. A single white pumice fragment from this layer yields 64 wt.% SiO_2 (Fig. 5), and has a mineral assemblage similar to that of the N2 pumices. This layer is overlain by an 18-cm-thick organic-rich soil, whose base has been dated at 8860±70 yr BP, indicating that the N3 tephra is slightly older than this age.

2.2.4. N4 tephra layer

The N4 tephra layer at SA-67 section is a 43-cm-thick fine greenish ash layer containing plagioclase and quartz crystals, fragmented lithics and 1–2 mm gray pumices, with rare 2–3 cm pumices scattered throughout this deposit. It is overlain by a 146 cm brown dark paleosol containing amphibole-rich yellow pumices at the base. The top of this deposit has been strongly weathered and is partially transformed into a brown soil. Pumices from this N4 layer yield 62 wt.% SiO_2 (Fig. 5) and have a mineral assemblage comprised of plg+opx+amph+Fe–Ti oxides.

2.2.5. N5 tephra layer

In section SA-67 (Fig. 4), N5 fallout is a 23-cm-thick well-sorted layer composed of 2–4 cm sub-angular yellow/orange pumices, gray angular lithics, as well as hydrothermally altered lithics (1–2 cm in diameter). The matrix constitutes 20% of the deposit and is composed of coarse ash (plagioclase, amphibole and glass shards). In sections SA-38 and SA-34 (Fig. 4), this layer has a thickness of 50 and 103 cm, respectively. In section SA-34 (which lies along the axis of dispersion, see below), this layer shows an oscillatory grading, being inverse at the base of the layer and changing to normal grading from the middle of the deposit to the top. The pumices reach a maximum of 7 cm in diameter with an average diameter of 3–4 cm. Abundant (30%) 2–3-cm reddish hydrothermally altered dacitic lava lithics are present. In this section, the fallout deposit is overlain by 10 cm of brown fine ash, and a paleosol horizon with variable thickness (22–30 cm). Silica contents of analyzed pumices ranges from 61 to 63 wt.%, with a mineral assemblage bearing plg+amph+opx+Fe–Ti oxides. In section SA-38 (Fig. 4), a 70-cm-thick dark paleosol underlies the N5 fallout, the upper part of the paleosol yields an age of 4600±40 yr BP.

2.2.6. N6 tephra layer

In section SA-67, the N6 fallout deposit is a well-sorted 45-cm-thick layer (Fig. 4). It is dominantly made up of sub-angular 2–5 cm

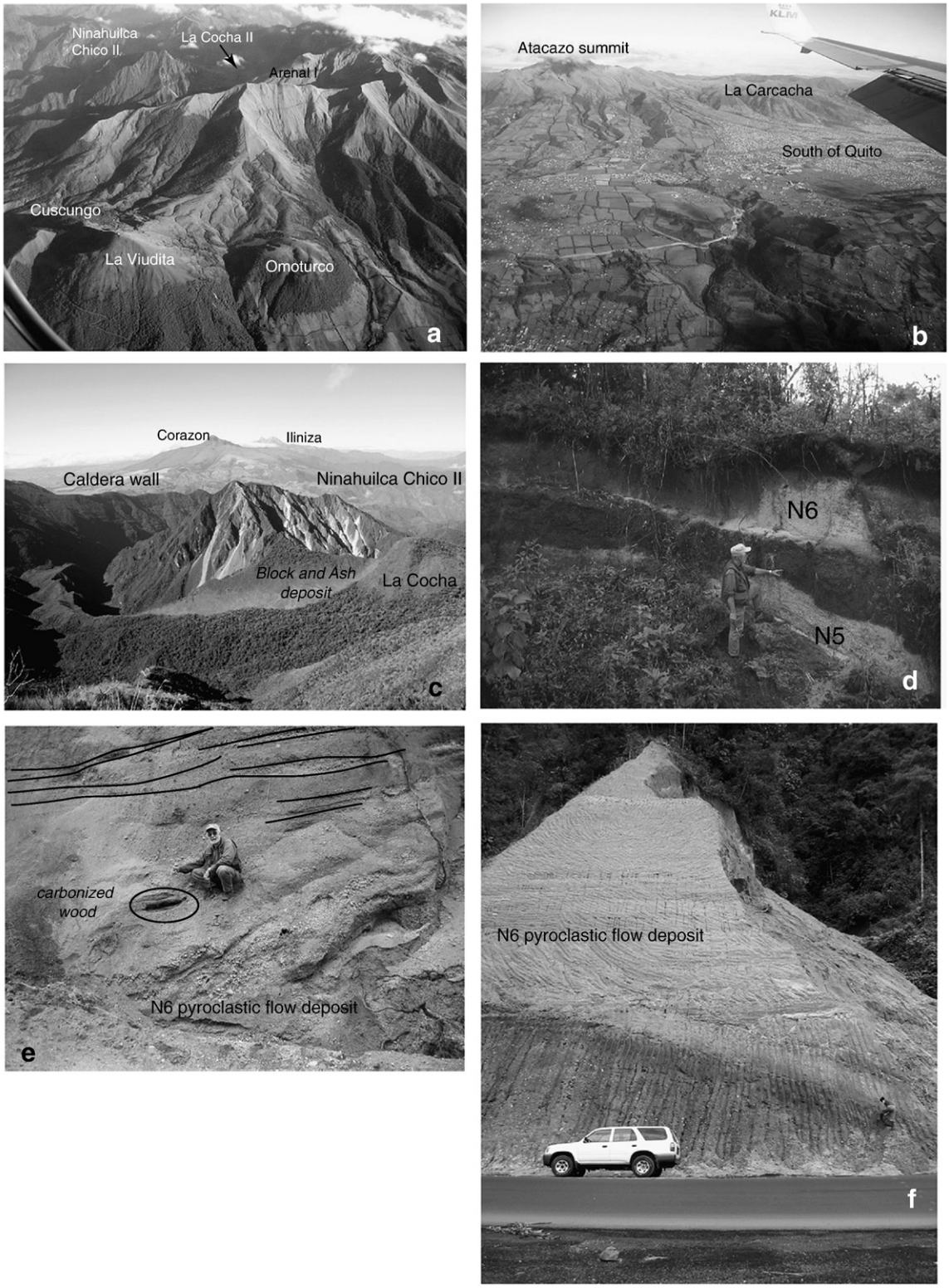

Fig. 3. a. ANVC aerial view from the SE. The southern external domes Omoturco, Cuscungo, and La Viudita appear in foreground; Arenal I, La Cocha II and Ninahuilca Chico II appear behind ancient Atacazo lavas. b. La Carcacha and Atacazo ancient edifices and the highly populated area of the south of Quito. c. La Cocha and Ninahuilca Chico II domes inside the Atacazo depression. d. N5 and N6 plinian fallout deposits (Section SA-34). e. N6 pyroclastic flow deposits at 6 km from the vent (Section SA-42). Note the large amount of carbonized material found inside these deposits. f. N6 pyroclastic flow deposits at 16 km from the vent (Section SA-22).

white/yellow pumices with some scattered pumices up to 10 cm in diameter. Gray and/or reddish hydrothermally altered lithics (2–3 cm) are also present. The matrix is coarse ash formed by plagioclase, amphibole and glass shards. In section SA-34 (Figs. 3d and 4), this layer overlies a dark paleosol of variable thickness and is capped by the modern soil.

This deposit is best exposed 5 km southwest of the vent (Ninahuilca Chico II), in the zone of Canchacoto (section SA-36; Fig. 4). At this

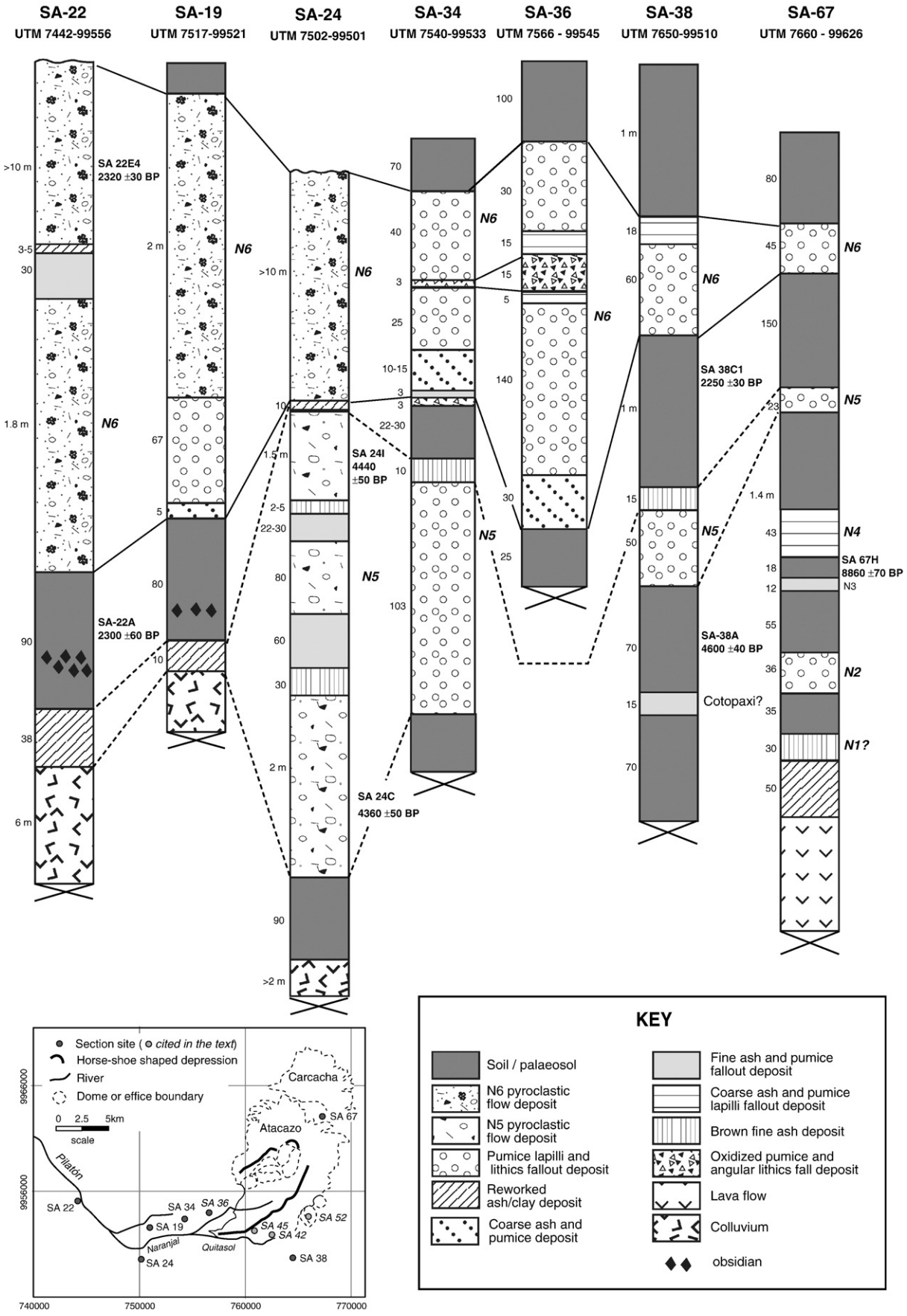

Fig. 4. Locations and stratigraphic correlations of the seven most representative sections of the recent ANVC pyroclastic deposits. Cotopaxi and GP (Guagua Pichincha) refer to fallouts from these two volcanoes. Thickness of the units is given in centimeters (except where indicated in meters). The new radiocarbon ages are also shown. Inset: Location of sections SA-42, SA-45 and SA-52 (cited in the text).

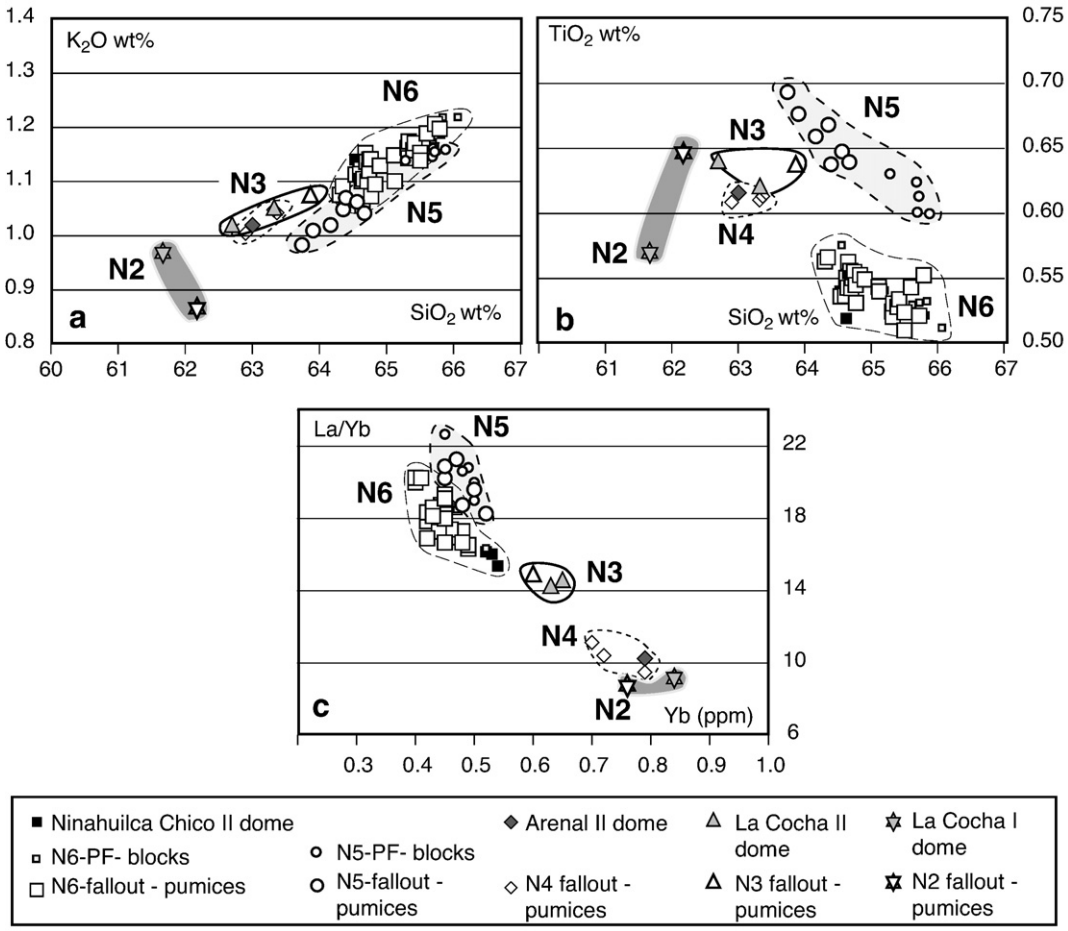

Fig. 5. Diagrams a. K_2O b. TiO_2, vs. SiO_2 and c. La/Yb vs. Yb diagrams, showing the geochemical relations between tephra layers pumices, blocks and pumices from the pyroclastic flow deposits, and intra-depression lava domes.

location, the deposit is 240 cm-thick and preserves a complete eruptive sequence. At the base of the deposit lies a 30 cm coarse ash and pumice layer, rich in 1-mm-size fragmented crystals of plagioclase, amphibole, Fe–Ti oxides, subordinate orthopyroxene, glass shards and sub-angular tiny pumices. This ash and pumice layer is conformably overlain by a 140-cm-thick reverse graded tephra fallout deposit, in which angular white pumices (65% of the deposit) reach a maximum diameter of 7 cm, and an average diameter of 2 cm. Angular gray and reddish hydrothermally altered lithics are also present (5%; 3–4 cm of maximum diameter). The matrix (30% of this layer) is made up of plagioclase, amphibole, Fe–Ti oxides crystals, glass shards, tiny crushed pumices and fragmented lithics.

Overlying the pumice fallout layer is a 5-cm-thick gray-greenish coarse ash and pumice fallout. Its composition is the same as that of the previous layer matrix. Rare pumice clasts may reach 1 cm in diameter. This layer is overlain by a 15-cm-thick fallout deposit which is comprised of regular 2–4 cm angular pumices (40%) and reddish hydrothermally altered lithics (almost 30%). The matrix (30%) is similar to that of the previous layer. Clasts from the top five centimeters of this layer are typically 1–1.5 cm in diameter. A 15-cm-thick layer of coarse ash and pumices overlies the lithic-rich layer. This gray-brown ash is comprised of plagioclase, amphibole, Fe–Ti oxides crystals, glass shards, fragmented pumices and lithics. Pumices in this layer do not exceed 1 cm.

At the top of the section, there is a brown-yellow 30-cm-thick reverse graded tephra fallout deposit. Light yellow pumices (50% of the deposit) reach maximum diameters of about 6 cm, they have a range of 62 to 65 wt.% SiO_2 and a mineral assemblage similar to N5 pumices with the addition of scarce apatite. Angular gray lithics make up 5–10% of the deposit. Their diameters do not exceed 2 cm. Reddish hydrothermally altered lithics are less common than in the previous layers. The fallout matrix is gray-brown coarse ash.

A sample of the paleosol directly beneath the tephra fallout deposit in section SA-38 yields an age of 2250±30 yr BP.

2.3. Pyroclastic flow deposits

2.3.1. N4 — ash-flow deposit

This deposit underlies N5 tephra fallout in section SA-30 (20 km SW of the Atacazo depression center). Its thickness is about 80 cm and most of the deposit has almost completely degraded into soil. Nevertheless, scarce plagioclase and amphibole crystals, tiny pumices and carbonized leaves are still distinguishable from the surrounding matrix. Indeed, the ubiquitous presence of the carbonized leaves and little charcoal pieces is the clue to recognize this deposit as an ash-flow. Carbonized material at the base of the deposit yields a ^{14}C age of 5440±110 yr BP (Almeida, 1996).

2.3.2. N5 — pyroclastic flow deposit

In section SA-24, the N5 eruptive period is represented by a gray-pink coloured ash-and-pumice deposit. The matrix forms 75% of the volume. It contains coarse-grained ash, rich in glass shards, crushed pumices and lithics, plagioclase, amphibole, quartz, and Fe–Ti oxides. Pumice blocks comprise 15% of the deposit while white andesitic and

dacitic lithics comprise 10%. Pumices blocks have 64 to 65 wt.% SiO_2, and the mineral assemblage of these rocks is the same as that of N5 tephra layer pumices.

This deposit is widely distributed around the Atacazo edifice, exposed in almost all the ravines with variable thickness (1–10 m) depending on the amount of erosion. Far to the southwest, the deposit filled the fluvial valleys of the Quitasol, Naranjal and Pilatón rivers, reaching maximum heights of about 120 m over the present day bottom of the valley, cropping out even near the town of Tandapi (section SA-24, Fig. 4). The flow is crudely stratified. Fine ash-rich layers are interbedded with lenses filled by rounded pumices of varying size (2–8 cm with rare 25 cm blocks) and oxidized clay-rich layers. Carbonized wood is abundant throughout the deposit. At section SA-24 the deposit overlies an ancient colluvium comprised of metamorphic blocks within a purple clay-rich matrix. The top of the section is crowned by an incipient soil. Two carbonized wood samples

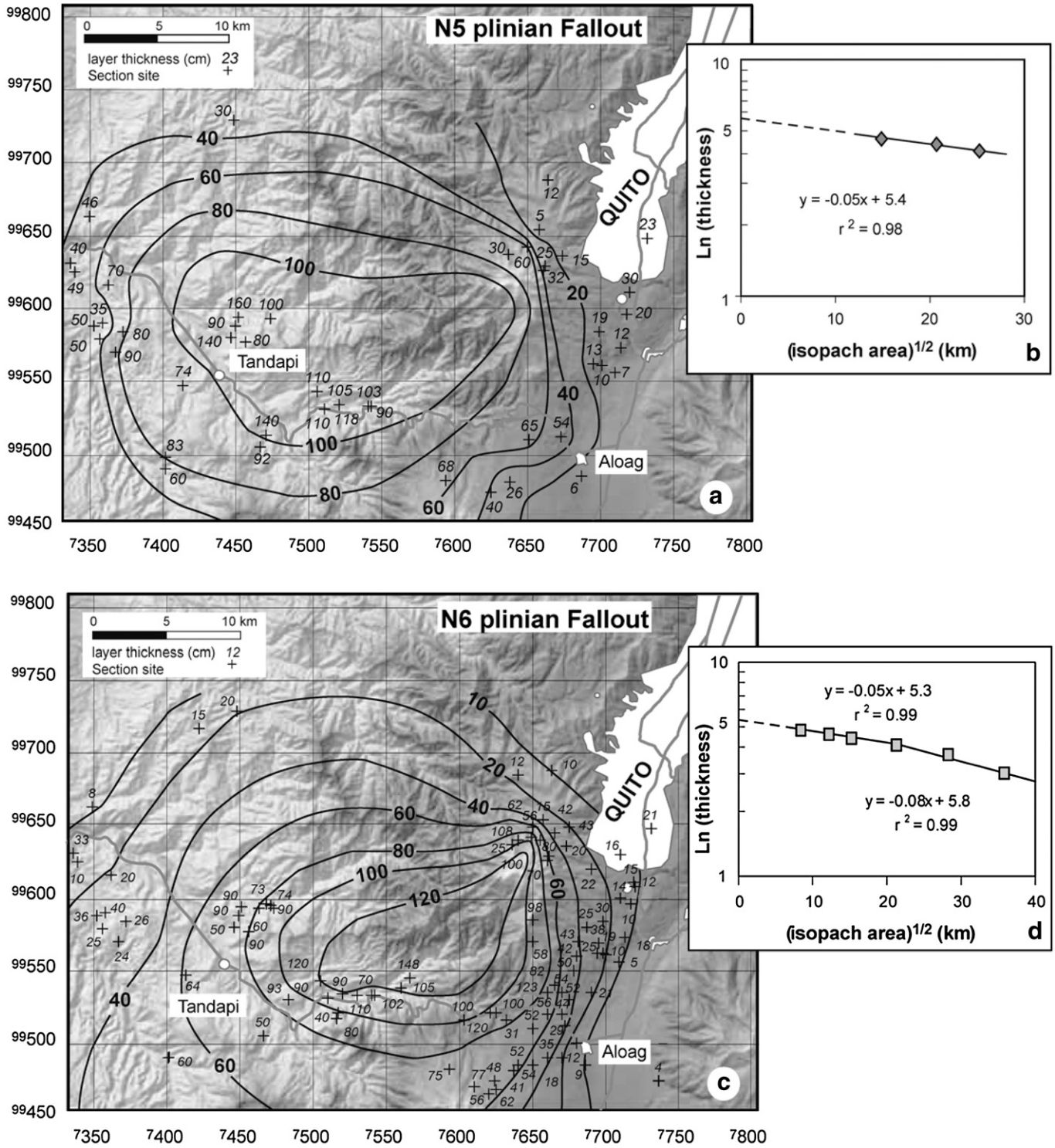

Fig. 6. a and c. Isopachs for N5 and N6 plinian tephra fallouts. Crosses indicate the sections where measurements were made. Thickness is indicated in cm. b and d. Ln (thickness) vs. Isopach area for N5 and N6 fallout isopachs, indicating the theoretical thinning of the deposits.

from this pyroclastic flow deposit yield coherent ages of 4360±50 and 4440±50 yr BP.

2.3.3. N6 — pyroclastic flow deposit

In several sections, the N6 eruptive period is represented by a deposit comprised by ash, pumices and dacitic blocks. This deposit corresponds to pyroclastic flows which are better preserved than those from the previous N5 period (Figs. 4 and 7). In general, the deposit appears light gray in colour. The matrix contains fine to coarse ash which is comprised of glass shards, tiny pumices, fragmented lithics, and crystals of plagioclase, amphibole, quartz, titano-magnetite and scarce ilmenite. The pumice block content is higher than in N5 deposits, reaching 20–30%, while the lithics (mainly dacitic lavas) content is of the same order (10%). Silica content of pumice clasts are around 64 wt.%, with a mineral assemblage of plg+amph+opx+Fe–Ti oxides±apt.

Those deposits cropping out in the areas close to the Ninahuilca Chico II dome (6 km from the dome Fig. 3e, SA-42) are crudely stratified with lenses of rounded pumice completely fines depleted. These were likely emplaced by grain-flow regimes (Hunter, 1985). Far to the west (16 km from the dome; Fig. 3f), on the Tandapi–Santo Domingo road (60 m above the Pilatón valley bottom; section SA-22; Fig. 4) the same pyroclastic flow deposit contains several fine ash and clay layers that define vague stratifications (Fig. 3f). At SA-19 (Fig. 4) the flow overlies the N6-plinian fallout, which in turn reposes over a dark brown paleosol horizon.

Carbonized wood was sampled from four different outcrops and yield ages of 2220±40 yr BP (section SA-42), 2230±40 yr BP (section SA-52), 2260±30 yr BP (section SA-45) and 2320±30 yr BP (Fig. 4, section SA-22). Charred twigs from the paleosol horizon underlying the pyroclastic flow deposit in section SA-22 yield an age of 2300±30 yr BP.

3. Correlating tephra layer deposits to late Pleistocene to Holocene intra-depression domes

Pumices sampled from the fallout layers and pyroclastic flow deposits can be correlated to the late Pleistocene–Holocene lava domes via whole-rock major and trace-element chemistry and mineralogical composition. Overall, there is an increase in silica as well as other major and trace elements from older to younger units (Fig. 5). As a result, several trace elements (for instance La/Yb, Fig. 5) have proven to be very useful in discriminating between each unit.

La Cocha I dome is an andesitic lava (61.3 wt.% SiO_2) with distinctively low K_2O and TiO_2 contents and La/Ce and La/Yb ratios relative to the other units (Fig. 5). Pumice from the N2 tephra layer plots similarly, except for TiO_2, whose concentration is a little higher in the tephra pumice. Mineral assemblages are the same for the dome and pumices samples, further corroborating the link between N2 tephra layer and La Cocha I dome.

La Cocha II dome rocks have medium K_2O and TiO_2 contents with La/Yb ratios around 14, (Fig. 5). These lavas are plg+opx+cpx+Fe–Ti oxides-bearing andesites and dacites. Their chemical compositions and mineral assemblage are similar to that of the N3 pumice. A slight positive correlation is observed in K_2O vs. SiO_2 plots. Although N2 and N3 pumices have similar mineral assemblages, the whole-rock analyses show that they are chemically distinct.

Arenal II dome is composed of a medium-K, plg+amph+opx+Fe–Ti oxides-bearing dacitic lava. Mineral and chemical compositions are nearly identical to that of the N4 pumice (Fig. 5). Overall, the N4 pumices have a homogeneous composition similar in SiO_2 to that of La Cocha II dome, but slightly lower in TiO_2 and La/Yb ratios. Both, the dome lavas and the N4 pumice include amphibole, which appears for the first time in the sequence of tephra layers.

N5 tephra layer and pyroclastic flow deposit samples display the largest variation in SiO_2. The pumice clasts are medium-K amphibole-bearing dacites. Pyroclastic flow pumices have 1–2 wt.% higher SiO_2 contents relative to those in the tephra layer (Fig. 5). Mineral assemblage is comprised of plg+amph+opx+Fe–Ti oxides. No correlation could be established between these products and any of the intra-depression domes. Nevertheless, given that the only dome not sampled in this study is Ninahuilca Chico I, and tephra grain size argues for a local source, we strongly suspect a link between this dome activity and N5 eruptive period. Additionally, the relative chronology of dome emplacement suggests that Ninahuilca Chico I formed before Ninahuilca Chico II, supporting the contention that this dome could have been related to N5 eruptive period deposits.

Ninahuilca Chico II lavas are medium-K amphibole-bearing dacites with a homogeneous composition. N6 tephra and pyroclastic flow samples overlap Ninahuilca Chico II dome chemical and mineralogical compositions. Samples vary in composition from 64 to 66 wt.% SiO_2 (Fig. 5). In the field, these rocks are quite similar to N5 period products; nevertheless, they can easily be distinguished from each other by their different TiO_2 contents.

4. Discussion

4.1. Tephra distribution and volumes of the last two eruptions

4.1.1. Fallout axes

The older N1 to N4 fallouts are so poorly exposed that no isopachs map could be drafted for these deposits. Three approximate isopachs (100–80–60 cm) have been drawn for N5 fallout deposits, while five better constrained isopachs (120–100–80–60–40 cm) have been produced for the most recent N6 sequence (Fig. 6). However, thinner deposits, important in the calculation of tephra volumes were not found in the studied area, so the estimations of tephra volumes does not include the distal fine ash that may account for an important part of the total volume. In both cases, fallout axes are oriented to the WSW, consistent with the known dominant wind direction in the region.

4.1.2. Tephra volumes

Isopach maps were used to calculate tephra volumes for N5 and N6 plinian fallouts using the equation of Pyle (1989), $V=13.08\ T_o(b_t)^2$, where V is the total volume of tephra, T_o is the maximum theoretical thickness of the deposit extrapolated after plotting the logarithm of isopach thickness versus the square root of the area enclosed by that isopach, and b_t is the thickness half distance along minor axis of the isopach plot (Table 2). Another formulation, that of Legros (2000), $V=3.69t_iA_i$, which uses only one isopach surface (A_i) and its thickness (t_i), was also used for comparison with the first estimation (Table 2). It is important to note that only minimal volumes could be estimated using this last formulation. In order to accurately determine the N6 plinian fallout volume, we used the approach from Fierstein and Nathenson (1992), which integrates with respect to the depositional area in order to accommodate irregularly shaped isopachs. All the resulting volumes are shown in Table 2. For N5 plinian fallout deposit, both volume calculations yield consistent results (1.7 km^3 using Pyle's formulation and 1.4 km^3 using Legros's equation). For N6 deposit, Legros (2000), Fierstein and Nathenson (1992) and Pyle (1989) approaches also produced consistent results (1.3, 1.2, and 0.9 km^3, respectively).

Table 2
Parameters used in the calculation of N5 and N6 plinian fallout volumes and volume estimations using different formulations (Pyle, 1989; Fierstein and Nathenson, 1992; Legros, 2000)

Eruptive period	T_o (cm)	B_t (km)	H_B (km)	V (km^3) (Pyle, 1989)	V (km^3) (Legros, 2000)	V (km^3) (Fierstein and Nathenson, 1992)
N5	211	7.93	35	1.7	1.4	–
N6	191	5.98	30	1	1.2	1.3

Column heights (HB) are also shown. See text for explanations.

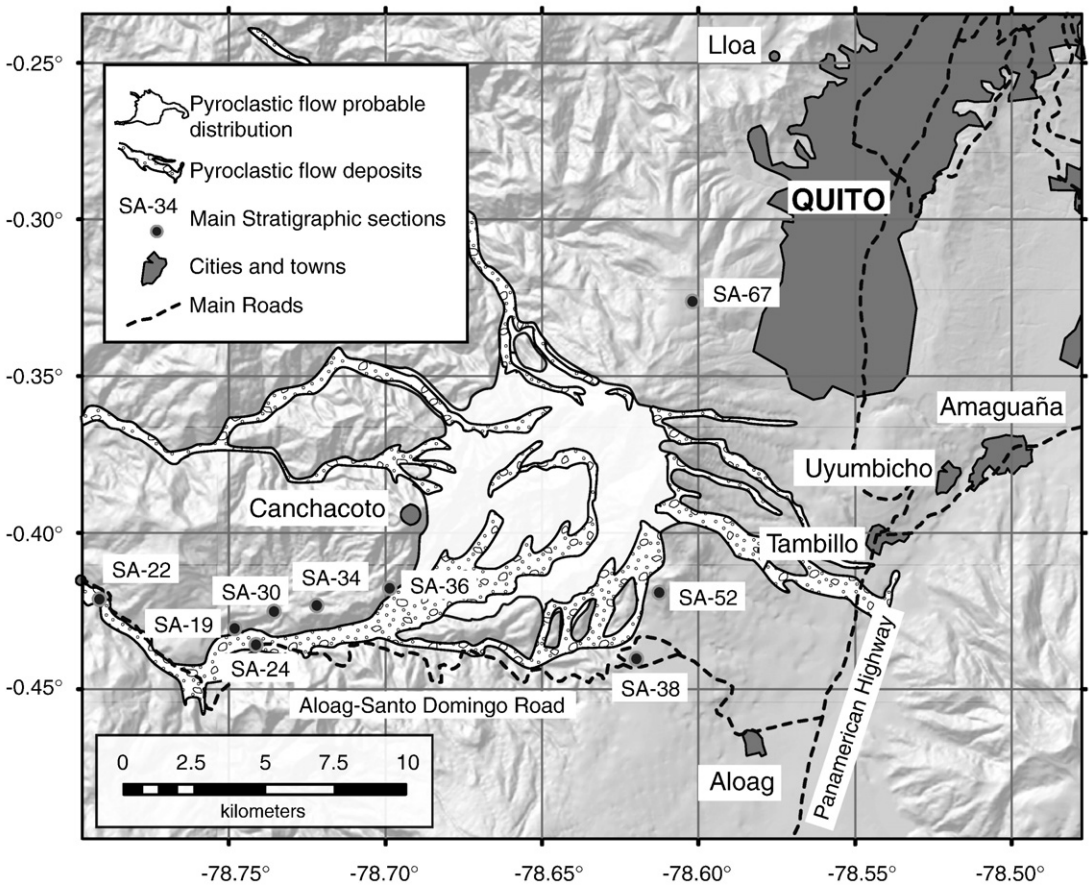

Fig. 7. Distribution of N6 pyroclastic flow deposits. Shown in white is the probable distribution based on VolcFlow simulation (Kelfoun and Druitt, 2005), while shown in circles filled pattern are the pyroclastic flow outcrops distribution based in Almeida (1996) and our own fieldwork. Notice that probable distribution is covered on the valleys by the actual outcrops.

Column heights for these two eruptions were estimated by Almeida (1996) at 35 km for N5 and 30 km for N6. These values are quite high and may result from an overestimation related to the use of the largest diameter of pumices and lithics instead of the average of three sides of each element (MP and ML). Assuming an overestimation of 20%, the eruptive columns still reach significant heights (>20 km). Combining these two parameters, the column height and tephra volume, a VEI (Volcanic Explosivity Index; Newhall and Self, 1982) of 5 has been assigned to both the N5 and N6 eruptions. These estimates and the characteristics of both fallout deposits, confirm the plinian character of these eruptions.

4.2. Pyroclastic flow deposits distribution and volumes

Few accessible outcrops combined with the severe erosion of the N5 and N6 pyroclastic flow deposits have greatly inhibited mapping of the distribution of these deposits. With the aim of constraining the distribution of pyroclastic flow deposits, a numerical simulation of these events has been done. Fig. 7 shows the probable original distribution of the deposits using the VolcFlow algorithm (Kelfoun and Druitt, 2005), which is a dynamic model that makes simulations of dense isothermal volcanic flows, based on the depth-average solution of the granular flow equations.

The distribution of pyroclastic flow deposits allows for the estimation of the probable volume of the N6 flow deposit. With an average thickness of 10–20 m and a maximal coverage area of 41 km^2, the total estimated volume is 0.4 to 0.8 km^3. This additional volume was taken into consideration when assigning a VEI of 5 to the N6 eruptive period.

4.3. Recurrence interval

Chronological data obtained for N6 deposits yield an age of 2270 ± 15 yr BP (between 400 and 230 BC calibrated ages with 2 sigma confidence level). The soil underlying the N5 plinian deposits is older than the average age obtained from the carbonized wood in the N5 pyroclastic flow deposit (Section SA-24). This average age yields 4440 ± 35 yr BP (between 3270 and 2910 BC). We have assigned ages of 5440 ± 111 yr BP (4500–3990 yr BC) to N4 (Almeida, 1996) and >8860 ± 70 yr BP (8240–7750 yr BC) to N3 (age of the soil over N3 fallout). Given that N2 tephra layer overlies Late glacial moraines, related activity could have taken place between 12 kyr and ≈8 kyr ago. Based on these dates, the eruptive recurrence interval ranges from about 1000 yr between N4 and N5 to 2700 yr between N5 and N6, and ≈3700 yr for the period N4–N3.

5. Conclusions

ANVC shows a recurrent pattern of explosive activity during the late Pleistocene and Holocene times. Six tephra layers (N1 to N6) have been described, and based on geochemical and petrographical descriptions; a correlation between tephra layers and the younger domes of the complex has been established.

The fallout and pyroclastic flow deposits described in this study confirm that all the Holocene eruptions of the ANVC were highly explosive plinian events. The volcanic explosivity index of the N5 and N6 eruptive periods (VEI = 5) exceeds that of all of the most violent eruptions of the last century in Ecuador. The deposits produced by the last two eruptions of ANVC (N5 and N6) underlie presently inhabited

areas with total populations of about 70 000, to the south of Quito, Tambillo, Uyumbicho, Aloag, Tandapi, and are exposed along part of the main highway linking the northern highlands to the coastal regions (Aloag–Santo Domingo road) as well as the Pan-American Highway. Should ANVC reactivate, it will compromise the National electrical infrastructure and part of the water supply for the southern Quito area. Fine ash distribution could have regional implications.

The combination of the few available chronological data from the literature with the ten new ages provided here shows that, for the recent volcanic activity, the recurrence period between eruptions is on the order of a few thousand years, ranging from about ~1000 yr to ~3700 yr. Considering the typical quiescence period of 1000–4000 yr between eruptions, and the age of the last recognized activity (2270± 15 yr BP), the possibility of a new eruption is increasing. As a result, mitigation plans should be elaborated and the hazard map improved. Additionally, a basic monitoring system should be deployed to look for signs of unrest at ANVC. An early warning system could help authorities to better handle a potential volcanic crisis, mitigating the effects of a new eruption for the population, the infrastructure and economic activities developed near the volcano.

Acknowledgements

This study benefited from the financial support of the IRD (Institut de Recherche pour le Développement, France), FUNDACYT (Fundación para la Ciencia y la Tecnología, Ecuador), and the French Embassy in Ecuador. Collaboration from the Departamento de Geofísica de la Escuela Politécnica Nacional was much appreciated. Our deepest thanks go out to Marc Souris and Jorge Aguilar for providing the data and generating the ANVC DEM. We thank Karim Kelfoun for his invaluable help in the modelling of the distribution of pyroclastic flow deposits. Whole-rock analyses have been carried out at the Université de Bretagne Occidentale by Joseph Cotten, whom we deeply acknowledge. Comments from Jean-Luc Le Pennec aided us in the development of this manuscript. Special thanks to Judy Fierstein and an anonymous reviewer whose comments greatly improved this paper.

References

Almeida, E., 1996. Dinámica de las Erupciones del Volcán Ninahuilca. 7° Congreso de Geología, Minas, Petróleo y Medio Ambiente, Quito.
Aquater, 1980. Informe geovolcanológico, Proyecto de investigación Geotérmica de la República del Ecuador, Estudio de Reconocimiento. Informe preparado por Aquater y BRGM para OLADE e INECEL, inédito. 54 p.
Barba, D., Robin, C., Samaniego, P., Eissen, J.P., 2008. Holocene recurrent explosive activity at Chimborazo volcano (Ecuador). Journal of Volcanology and Geothermal Research 176, 27–35 (this issue).
Barberi, F., et al., 1988. Plio-Quaternary volcanism in Ecuador. Geological Magazine 125 (1), 1–14.
Bronk Ramsey, C., 2003. OxCal v. 3.9, Oxford.
Clapperton, C.M., 1993. The Quaternary Geology and Geomorphology of South America. Elsevier, Amsterdam.
Fierstein, J., Nathenson, M., 1992. Another look at the calculation of fallout tephra volumes. Bulletin of Volcanology 54, 156–167.
Hall, M.L., 1977. El Volcanismo en el Ecuador. IPGH. Instituto Geográfico Militar, Quito. 120 pp.
Hall, M.L., Beate, B., 1991. El volcanismo Plio-Cuaternario en los Andes del Ecuador. In: Mothes, P. (Ed.), El Paisaje Volcánico de la Sierra Ecuatoriana, Quito, pp. 5–18.
Hall, M.L., Maruri, W., 1992. Mapa de los peligros volcánicos potenciales asociados con el Volcán Ninahuilca, Provincia de Pichincha. Instituto Geofísico — Escuela Politécnica Nacional, Quito.
Hall, M., Mothes, P., 1994. Tefroestratigrafía Holocénica de los Volcanes Principales del Valle Interandino, Ecuador. Estudios de Geografía 6, 47–67.
Hunter, R.E., 1985. A kinematic model for the structure of lee side deposits. Sedimentology 32, 409–422.
INEC, 2001. Censo de población 2001, pp. http://www.inec.gov.ec/web/.
Kelfoun, K., Druitt, T., 2005. Numerical modeling of the emplacement of Socompa rock avalanche, Chile. Journal of Geophysical Research 110, B12202.1–12202.13. doi:10.1029/2005JB003758.
Legros, F., 2000. Minimum volume of tephra fallout deposit estimated from a single isopach. Journal of Volcanology and Geothermal Research 96, 25–32.
Newhall, C.G., Self, S., 1982. The volcanic explosivity index (VEI): an estimate of explosive magnitude for historical volcanism. Journal of Geophysical Research 87, 1231–1238.
Pyle, M., 1989. The thickness, volume and grainsize of tephra fall deposits. Bulletin of Volcanology 51, 1–15.
Samaniego, P., Monzier, M., Robin, C., Hall, M.L., 1998. Late Holocene eruptive activity at Nevado Cayambe Volcano, Ecuador. Bulletin of Volcanology 59 (7), 451–459.